Ecological Applications, 28(6), 2018, pp. 1459–1472

Forest restoration as a strategy to mitigate climate impacts on wildfire, vegetation, and water in semiarid forests

Frances C. O'Donnell,[1,5] William T. Flatley,[2] Abraham E. Springer,[3] and Peter Z. Fulé[4]

[1]*Department of Civil Engineering, Auburn University, Auburn, Alabama 36849 USA*
[2]*Department of Geography, University of Central Arkansas, Conway, Arkansas 72035 USA*
[3]*School of Earth Sciences and Environmental Sustainability, Northern Arizona University, Flagstaff, Arizona 86011 USA*
[4]*School of Forestry, Northern Arizona University, Flagstaff, Arizona 86011 USA*

Abstract. Climate change and wildfire are interacting to drive vegetation change and potentially reduce water quantity and quality in the southwestern United States, Forest restoration is a management approach that could mitigate some of these negative outcomes. However, little information exists on how restoration combined with climate change might influence hydrology across large forest landscapes that incorporate multiple vegetation types and complex fire regimes. We combined spatially explicit vegetation and fire modeling with statistical water and sediment yield models for a large forested landscape (335,000 ha) on the Kaibab Plateau in northern Arizona, USA. Our objective was to assess the impacts of climate change and forest restoration on the future fire regime, forest vegetation, and watershed outputs. Our model results predict that the combination of climate change and high-severity fire will drive forest turnover, biomass declines, and compositional change in future forests. Restoration treatments may reduce the area burned in high-severity fires and reduce conversions from forested to non-forested conditions. Even though mid-elevation forests are the targets of restoration, the treatments are expected to delay the decline of high-elevation spruce–fir, aspen, and mixed conifer forests by reducing the occurrence of high-severity fires that may spread across ecoregions. We estimate that climate-induced vegetation changes will result in annual runoff declines of up to 10%, while restoration reduced or reversed this decline. The hydrologic model suggests that mid-elevation forests, which are the targets of restoration treatments, provide around 80% of runoff in this system and the conservation of mid- to high-elevation forests types provides the greatest benefit in terms of water conservation. We also predict that restoration treatments will conserve water quality by reducing patches of high-severity fire that are associated with high sediment yield. Restoration treatments are a management strategy that may reduce undesirable outcomes for multiple ecosystem services.

Key words: climate change; ecological modeling; fire ecology; forest restoration; hydrology; LANDIS-II; sediment.

Introduction

Climate change is altering vegetation distributions and fire regimes in the western United States. Vegetation types are shifting to higher elevations (Allen and Breshears 1998), and wildfires are becoming more frequent and intense (Westerling et al. 2011). Wildfire and vegetation change interact, as forests are commonly replaced by sprouting shrub vegetation that is better adapted to higher temperatures and drier conditions following wildfire (Strom and Fulé 2007, Tarancón et al. 2014). High-intensity wildfires often lead to reductions in water quality from erosion and high sediment loads (Neary et al. 2009, Smith et al. 2011) and vegetation type conversions are expected to influence watershed output (Huxman et al. 2005). With water deficits expected for the western United Sates in the coming century (Woodhouse et al. 2010), it is important to understand the threats to forested watersheds.

Forest managers are attempting to reduce the risk and spread of high-severity wildfires through forest restoration using treatments such as tree thinning, prescribed burning, and managed wildfires to decrease tree density and fuel loads. Restoration treatments have been successful in restoring historical forest attributes and reducing the potential for high-severity fire under contemporary climate conditions (Fulé et al. 2012). However, the outcomes of restoration under future climate conditions are uncertain and it may be difficult to utilize prescribed fire due to climate change effects on fire season windows. Due to uncertainty, there is interest in management that focuses on maintaining ecosystem function and regional native biodiversity (Stephenson 2014, Golladay et al. 2016) rather than recreating a historic condition. The provisioning of plentiful, clean water for both environmental flows and human use is an important ecosystem function for many semiarid forests.

The forests of the United States provide a significant amount of surface water and groundwater supply to the country (Barr 1956), and the connection between watershed land cover and the magnitude and timing of surface water flows has long been recognized (Bosch and Hewlett 1982, Robles et al. 2017). Recent studies have highlighted the importance of ecosystem health in the contributing area of an aquifer for reliable groundwater resources (Scanlon et al. 2005, Wyatt et al. 2015). Wyatt (2013) found, from a systematic global literature review, an average of 0–50% initial increase in water yield in coniferous forests when basal area is reduced by 5–100%. Forest restoration is also expected to maintain water quality by reducing the risk of high-intensity wildfire. Substantial soil loss due to rill and gully formation

Manuscript received 2 January 2018; accepted 26 April 2018. Corresponding Editor: John Stella.
[5] E-mail: fco0002@auburn.edu

occurs after high-intensity wildfire (Neary et al. 2012), which can increase sediment loads in rivers and streams. Monitoring before and after the Cerro Grande Fire, which burned ponderosa pine and mixed-conifer forest in New Mexico, found that post-fire suspended sediment concentrations in ephemeral streams were more than 100 times higher than pre-fire levels (Malmon et al. 2007). Most measures of water quality, including concentrations of major ions and nutrients, turbidity, and pH, are significantly altered by wildfire for at least four months (Earl and Blinn 2003).

The potential for land cover change to impact water quantity and quality is especially high for karst aquifers. Flow through karst aquifers is characterized by a combination of fast flow traveling through sinkhole and cave networks (Lauber and Goldscheider 2014) and slow flow traveling through porous media. Due to the fast flow component, discharge from karst aquifers is more sensitive to perturbations in water quality (Vesper et al. 2001, Mahler et al. 2004). Localized disturbance around a sinkhole, such as a high-severity wildfire, is likely to degrade the quality of discharge from the connected fast flow karst system, Therefore, management of upland forests to preserve hydrologic function may be a feasible strategy for conservation of spring, aquatic, and riparian habitat that is supported by discharge from a karst aquifer.

The Kaibab Plateau, which forms the North Rim of Grand Canyon National Park (GCNP), is a classic representation of a snowmelt-dominated karst aquifer system (Tobin et al. 2017). Snowmelt runoff and precipitation infiltrates the Kaibab Plateau rapidly via sinkholes, faults, and fractures and slowly through diffuse infiltration. Once in the subsurface, it travels hundreds of meters vertically before moving laterally through the karst system in the North Rim's Redwall-Muav Aquifer (R-aquifer; Brown 2011, Jones et al. 2017). Sinkhole density on the Plateau is 3–5 sinkholes/km^2. Most precipitation (about 60%) falls during the winter (November–March) as snowpack and subsequently melts during spring (March–May), when low temperatures, minimal plant use, and saturated conditions in the vadose zone allow more water to recharge the aquifer system. Roaring Springs, the primary water source for GCNP, requires winter precipitation to sustain perennial flow as little recharge occurs during the summer monsoon (mid-July–September; Ross 2005, Schindel 2015). Most water discharged from the R-aquifer aquifer is relatively young and susceptible to rapid impacts from land-use activities on the Kaibab Plateau (Ross 2005).

We combine spatially explicit vegetation and fire modeling with statistical water and sediment yield models to evaluate the impacts of a range of restoration and climate scenarios on water inputs to a karst system. The study objectives were to (1) predict changes in fire regimes and forest vegetation on the Kaibab Plateau under a range of climate and restoration scenarios; (2) estimate the change in future hydrologic and sediment output due to forest type change and restoration; and (3) identify areas of the Kaibab Plateau that are most likely to experience negative hydrologic impacts.

Methods

Study site

The Kaibab Plateau is a 335,000-ha area of the Colorado Plateau region in Northern Arizona and includes portions of GCNP and the Kaibab National Forest (KNF). Elevation ranges from 1,439 to 2,830 m and climate and vegetation type vary with elevation. At Bright Angel Ranger Station, the only long-term climate monitoring site in the study area, average annual precipitation was 62.7 cm and temperatures ranged from an average July maximum of 25.2°C to an average January minimum of −8.1°C (NOAA NCEI 2011). About 40% of precipitation occurs as high-intensity summer monsoon storms and 60% occurs as low-intensity winter rain or snow. Most runoff and groundwater recharge on the southern Colorado Plateau are generated by winter precipitation (Baker 1986). Soils are primarily alfisols and entisols derived from limestone parent material (USDA NRCS 2013).

Variability of environmental site conditions and corresponding differences in species viability and growth are represented in LANDIS-II by subdividing the modeled landscape into ecoregions. We divided the Kaibab Plateau into four elevation-based ecoregions that align with the major forest types and associated fire regimes (Table 1): high elevation (spruce–fir; 2,675–2,830 m), high-mid elevation (mixed conifer; 2,450–2,675 m), low-mid elevation (ponderosa pine; 2,050–2,450 m), and low elevation (pinyon–juniper; 1,600–2,050 m; Vankat 2011*a*, *b*). We further diveded these elevation-based ecoregions by northeast- and southwest-facing aspects, resulting in a total of eight ecoregions. See Flatley and Fulé (2016) for a detailed description of the vegetation and fire regimes at the study site.

The Kaibab Plateau is uplifted to the East by the structural East Kaibab Monocline. After water infiltrates, dominantly through focused recharge in the over 7,000 sinkholes in the Permian Kaibab Formation, it travels vertically downward for hundreds of meters to the regional R-aquifer. The R-aquifer is composed of the Cambrian Muav Formation, Devonian Temple Butte Formation, and Mississippian Redwall Limestone and is perched on the Cambrian Bright

Table 1. Elevation range, dominant vegetation type, and climate for four ecoregions on the Kaibab Plateau, Arizona, USA.

Ecoregion	Elevation (m)	Dominant vegetation type	Annual precipitation (mm)	Maximum July temperature (°C)	Minimum January temperature (°C)
High	2,675–2,830	Spruce–fir	746	25.4	−9.8
High-mid	2,450–2,675	Mixed conifer	656	26.4	−8.7
Low-mid	2,050–2,675	Ponderosa pine	489	28.8	−6.7
Low	1,600–2,050	Pinyon–juniper	365	32.1	−4.7

Notes: Values are means. Precipitation and temperature values are derived from PRISM 30-yr climate normals for 1981–2010 (PRISM Climate Group 2004).

Angel Shale. North Rim springs are a mix of older water from groundwater storage and younger water from fast karst recharge (Monroe et al. 2004). Although there are over 20 springs, most of the water discharges from Angel Spring, Emmett Spring, Roaring Spring, Abyss Spring, Tapeats Spring, and Thunder River Spring (Jones et al. 2017).

Climate and restoration scenarios

We simulated the response of wildfire, forest dynamics, and hydrologic output to changes in climate and restoration approaches from 2010 to 2110. Each simulation included an initialization run up of 600 yr under the historical fire regime (calendar years 1280–1880), followed by 130 yr of fire exclusion (calendar years 1880–2010), which allowed forest conditions to reach a state that approximates current forest conditions within the study area (see Flatley and Fulé 2016). The impact of 20th century logging within the (KNF) was simulated with two logging treatments implemented with the biomass harvest extension (v2.1; Gustafson et al. 2000). Based on timber records from the forest (Sesnie and Bailey 2003), we applied a selective logging treatment that removed 25% of the biomass from all cohorts across a cumulative 50% of the landscape during 1955–1980. Then we applied a more intensive logging treatment that removed 50–70% of the biomass from mature cohorts (>31 yr), across a total of 24% of the landscape from 1980 to 1990. Logging treatments were not applied to forests in GCNP, reflecting the absence of past logging in these forests. We then modeled the landscape response according to a series of climate and restoration scenarios spanning 2010–2110. We ran 10 replicates for each scenario in order to account for stochasticity associated with individual fire events that vary according to ignition points and fire weather in individual runs.

We modeled nine future change scenarios (3 climate scenarios $\times$ 3 restoration scenarios) designed to assess the outcomes of changing climate and restoration approaches alone and in combination. Future climate projections were based on an ensemble average of 17 general circulation models (GCM) included in the IPCC fifth assessment and available for use with Climate-FVS (Crookston and Rehfeldt 2008). We chose the ensemble GCM outputs from representative concentration pathway (RCP) 4.5 as an assessment of moderate climate change and RCP 8.5 as a high climate change scenario (Meinshausen et al. 2011). We initiated climate-induced growth and establishment changes in 1990 for both the RCP 4.5 and RCP 8.5 climate change regimes, while we held the historical climate conditions constant for the no climate change regime.

We tested three restoration scenarios that differed in terms of the area treated annually: no restoration, low restoration, and high restoration. The no restoration scenario included no thinning or burning. The low and high restoration scenarios implemented thinning treatments for an initial 20 yr (1990–2010), followed by prescribed burning for the remainder of the simulation. The modeled restoration treatments match contemporary restoration practices in southwestern frequent-fire forests in which thinning is used to alter forest composition and structure, followed by prescribed burning for the reduction of fuel loads (Reynolds et al. 2013). We only applied restoration treatments in the low-mid-elevation and high-mid-elevation ecoregions, which are currently occupied by ponderosa pine and dry-mixed conifer. The low restoration scenario treated 1.25% of the target area per year (80-yr rotation) with thinning or prescribed burning and the high restoration scenario treated 5% of the target area per year (20-yr rotation).

Vegetation modeling approach

Climate-FVS and LANDIS-II.—We used Climate-FVS and LANDIS-II to model fire regime and forest response to climate change and restoration treatments. Climate-FVS is a forest growth simulation model that adjusts species viability and growth rates according to site specific, downscaled climate projections (Crookston et al. 2010). We used Climate-FVS to estimate input values for LANDIS-II, which included species establishment probabilities, aboveground net primary productivity, and maximum aboveground live biomass for individual species in response to changing climate conditions. LANDIS-II (v6.0; Scheller et al. 2007) is a spatially interactive forest landscape simulation model that can be used to model spatial processes such as fire spread, forest succession, and species dispersal (Gustafson et al. 2010, Duveneck and Scheller 2015, Hurteau et al. 2016). The core model is compatible with a series of extensions for simulating forest processes. We modeled forest growth, competition, succession, and regeneration using the Biomass Succession extension (v3.1; Scheller and Mladenoff 2004). We chose a 1-ha cell resolution, with each of the extensions operating at a 5-yr time step. Flatley and Fulé (2016) provide a detailed description of the model structure and calibration for the Kaibab Plateau study area (see Appendix A in Flatley and Fulé [2016] for LANDIS-II input parameters).

Fire disturbance.—We used the Dynamic Fire and Fuels System (DFFS) extension for LANDIS-II (v2.0; Sturtevant et al. 2009) to model fire disturbance. DFFS simulates fire occurrence and spread according to inputs of daily fire weather data, ignition rates, and fire duration distributions that vary by ecoregion. We collected daily fire weather data (ca. 1995–2013) for each ecoregion, including temperature, wind speed, wind direction, relative humidity, and precipitation, from seven Remote Automated Weather Stations (RAWS) located within or adjacent to the study area and available for download through the Western Regional Climate Center (available online).[6]

We calibrated the parameters for the historical fire regime, used during the initialization period prior to the future change scenarios, according to historical mean fire intervals from local tree ring reconstructions of fire history. We modeled the baseline (no climate change) future fire regime according to mapped fire perimeters within GCNP from 1990 to 2011. We removed all prescribed fires from this list, then grouped the fires according to the ecoregions in which they occurred. We then used the list of fires to calculate fire size parameters for each ecoregion. We iteratively adjusted the initial fire size parameters according to the results of calibration runs on the full landscape until mean fire size and fire rotations in each ecoregion approximated those

[6] http://www.raws.dri.edu.

calculated from the initial federal fire records. We then used fire durations provided in the DFFS output for each fire to create fire duration distributions for each of the calibrated fire regimes. The use of a fire duration rather than fire size to parameterize the fire regime allows fire sizes to respond to future changes in fire weather resulting from climate change. For example, climate change influences on fire weather may increase the rate of fire spread, allowing a fire to burn more area during the same fire duration period.

We simulated fire regime response to future climate change by adjusting daily fire weather data according to projected shifts in temperature and precipitation for each climate scenario (RCP 4.5 and RCP 8.5) and each time step for which projections were available (2030, 2060, and 2090). We added projected temperature increases directly to daily temperature values and multiplied daily precipitation values by the projected percent change in annual precipitation. We adjusted daily relative humidity values according to increased temperature effects on atmospheric water vapor capacity but did not factor precipitation changes into relative humidity values. Precipitation changes were relatively minor under both climate change scenarios (1–6% percent change). Fire spread rates responded to fire weather changes, resulting in increases or decreases in area burned and fire severity. Fire severity is calculated according to fire spread rate, foliar moisture content, and the fuel type parameters of crown base height and surface fuel consumption (Sturtevant et al. 2009).

Restoration treatments.—We implemented restoration treatments (thinning and prescribed burns) with the Biomass Harvest extension. Restoration treatments were based on thinning and prescribed burn treatment prescriptions obtained from staff with the KNF and GCNP. In the low-mid elevation ecoregion, thinning treatments removed cohorts of all species except *Pinus ponderosa* and *Quercus gambelli*. *P. ponderosa* and *Q. gambelli* cohorts younger than 110 yr (i.e., cohorts that established after fire exclusion) had their biomass reduced by 80–95%. We implemented the prescribed burns in the Biomass Harvest extension, because the DFFS extension is designed to simulate a relatively stochastic wildfire regime. The Biomass Harvest extension enables the user to control the total area impacted and target individual stands as managers would with a prescribed fire. In the low-mid-elevation ecoregion, we implemented prescribed burns to remove cohorts of all species except *P. ponderosa* and *Q. gambelli*. We reduced ponderosa cohorts in biomass according to their age (1–10 [95% biomass removed]; 11–30 [80%]; 31–100 [50%]; 101–1,000 [10%]). *Q. gambelli* cohorts <100 yr old had their biomass reduced by 95%. In the high-mid-elevation, we only applied thinning and prescribed burning treatments to south and west-facing aspects. For thinning treatments, *Abies concolor*, *Pseudotsuga menziesii*, *P. ponderosa*, and *Q. gambelli* cohorts were retained, with biomass reductions matching those in the low-mid-elevation prescribed burns. Prescribed burns retained cohorts of these same species, with the same age related biomass reductions used for the low-mid-elevation prescribed burns. Following a thinning treatment or a prescribed burn, we assigned cells to the post-fire fuel type for the next 20 yr (Yocom 2013).

Vegetation model outputs.—LANDIS-II model runs produced raster maps of individual tree species biomass at 10-yr time steps which we then converted to maps of forest types and basal area for input into the hydrologic model. We created forest type maps with the Biomass Reclass extension, using individual tree species biomass to classify raster cells into the following forest types: spruce–fir (*Picea engelmannii*, *Abies lasiocarpa*, *Picea pungens*), aspen (*Populus tremuloides*), wet mixed conifer (*A. concolor*, *P. menziesii*, *P. engelmannii*, *A. lasiocarpa*, *P. pungens*), dry mixed conifer (*A. concolor*, *P. menziesii*, *P. ponderosa*), ponderosa pine (*P. ponderosa*), Gambel oak (*Q. gambelli*), pinyon–juniper (*Pinus edulis*, *Juniperus osteosperma*), and non-forest (no tree species biomass). Using previously collected, local plot data representing each of the modeled forests types, we developed relationships between individual species biomass and basal area (Fulé et al. 2002, 2003*a*, *b*, Huffman et al. 2008, 2009). We used allometric equations to calculate biomass by species for each plot in the data set (Chojnacky et al. 2014) and developed linear regressions relating plot level biomass to basal area for individual species. We used these regression equations to convert individual tree species biomass outputs from LANDIS-II to total basal area per cell.

The design of LANDIS-II around tree cohorts, rather than individual trees, presented a challenge in assessing the influence of forest structure on hydrologic output. The regression equations used to convert individual species biomass to basal area were robust (r^2 = 0.99–0.97). Yet, we recognize that a single basal area value could represent drastically different structures (e.g., many small diameter trees vs. a few large diameter trees). However, the basal area values were only used to estimate changes in runoff immediately following restoration treatments. Basal area removed during restoration treatments targeted younger cohorts. This would shift biomass and basal area towards older, larger cohorts, which should align well with the structural outcomes of treatments in the paired watershed experiments.

Hydrologic modeling approach

Rainfall–runoff equations.—We developed regression equations for the rainfall–runoff relationship in each of the major vegetation types on the Kaibab Plateau through a reanalysis of data from historic paired watershed studies conducted in Arizona in the 1950s–1980s. The existence of large historical data sets and lack of quality environmental forcing, calibration, and validation data for the site make a statistical modeling approach more appropriate than a process-based approach for surface hydrology on the Kaibab Plateau. Experimental logging treatments were performed on many of the watersheds (Baker 1999). We used pre-treatment and control watershed data to develop the rainfall–runoff relationships so that the relationships are representative of an undisturbed watershed. While the use of historical data does not account for the effects of fire suppression in the second half of the 20th century, an analysis of streamflow, climate, and forest cover from 1914 to 2012 found that the majority of streamflow declines attributable to fire suppression occurred between 1914 and 1963 (Robles et al. 2017). We normalized runoff by area to give units of depth and tested linear and quadratic rainfall–runoff functions for each ecoregion using

r^2 and root mean square error (rmse) to indicate the goodness of fit, and tested both winter (October–May) and total annual precipitation as explanatory variables. We included additional variables in the relationship and used an F test to determine if their coefficient values were significantly different from zero at the 95% confidence level. The additional variables tested included watershed size, slope and aspect, and mean, minimum, and maximum temperature both annually and during the winter. Precipitation was the only significant predictor of runoff. To test for model overfitting, we fit the equations to a random sample of 70% of the original data and tested for goodness of fit with the remaining 30% of the data. We examined model residuals for patterns of dispersion or bias. We conducted an independent validation of our model for runoff in undisturbed watersheds using data from two USGS gauging stations in the region with vegetation types similar to the Kaibab Plateau. We used gridded precipitation and vegetation data sets for model inputs. Modeled runoff provided a good fit ($r^2 > 0.83$) to measured data with no detectable bias. Full validation methods and results are presented in Appendix S1.

We determined the rainfall–runoff relationship for the high-elevation forest types, including wet mixed conifer, spruce–fir, and aspen, using data from the Thomas Creek and Willow Creek experimental watersheds on the Apache-Sitgreaves National Forest in east-central Arizona. The sites support a mix of wet mixed-conifer, spruce–fir, and aspen forest types. Willow Creek has one gauged watershed that ranges in elevation from 2,680 to 2,830 m, and mean annual precipitation is 863 mm (Gottfried 1983). Thomas Creek has one control and one treatment watershed that range in elevation from 2,545 to 2,819 m with an annual precipitation of 768 mm (Gottfried 1991). The two sources provide a total of 58 site-years of data and give a rainfall–runoff relationship of

$$\begin{aligned} R &= 0.000338P^2 + 0.00959P - 2.16, P \geq 67\,\text{mm} \\ r^2 &= 0.85, \text{rmse} = 66.5 \end{aligned} \quad (1)$$

where R is annual runoff and P is winter (October–April) precipitation, both expressed in mm.

We used data from the three gauged watersheds at Workman Creek Experimental Watershed to determine the rainfall–runoff relationship for the dry mixed conifer forest type. Workman Creek is located in dry mixed conifer forest in the Sierra Ancha Mountains approximately 100 km northeast of Phoenix at an elevation of 2,010–2,356 m with a mean annual precipitation of 835 mm (Rich and Gottfried 1976). The instrumentation consists of a main dam weir just below the confluence of the north, middle, and south forks of Workman Creek with weirs on the north and south forks just above the confluence that can be subtracted from the main dam flow to determine flow in the middle fork. Twenty-eight site-years of data are available and provide the relationship

$$\begin{aligned} R &= 0.295P - 80.3, P \geq 272\,\text{mm} \\ r^2 &= 0.89, \text{rmse} = 26. \end{aligned} \quad (2)$$

The Beaver Creek Experimental Watershed on the Coconino National Forest included 20 small, gauged catchments, six in the pinyon–juniper vegetation type and 14 in the ponderosa pine forest type. The catchments in the ponderosa pine type range in elevation from 2,054 to 2,225 m, and mean annual precipitation, measured by a network of gauges, ranges from 550 to 785 mm (Baker 1986). The pinyon–juniper catchments range in elevation from 1,580 to 1,950 m with mean annual precipitation of 304 to 685 mm (Clary et al. 1974). We developed the rainfall–runoff relationship for the ponderosa pine and oak forest types using data from ponderosa pine catchments at Beaver Creek and the Castle Creek Experimental Watershed in ponderosa pine forest in eastern Arizona. Castle Creek had a treatment and control pair of gauged watersheds at elevations of 2,390–2,600 m with a mean annual precipitation of 635 mm (Rich 1972). The 78 site-years of data for ponderosa pine give the following relationship:

$$\begin{aligned} R &= 0.591P - 139.8, P \geq 236\,\text{mm} \\ r^2 &= 0.85, \text{rmse} = 52. \end{aligned} \quad (3)$$

We used data from Corduroy Creek in eastern Arizona in addition to the pinyon–juniper catchments at Beaver Creek to develop a rainfall–runoff relationship for the vegetation type. Two branches of Corduroy Creek were gauged and range in elevation from 1,580 to 2,250 m with a mean annual precipitation of 508 mm (Collings and Myrick 1966). Based on 110 site-years of data, the rainfall–runoff relationship is

$$\begin{aligned} R &= 0.000425P^2 - 9.46, P \geq 149\,\text{mm} \\ r^2 &= 0.82, \text{rmse} = 18.2. \end{aligned} \quad (4)$$

While vegetation types characteristic of lower elevations than pinyon–juniper are not common on the Kaibab Plateau under current conditions, it is likely that non-forest vegetation types will become more common in the future due to climate change and fire. We developed a rainfall–runoff relationship to represent these vegetation types using data from two experimental watersheds in the chaparral vegetation type. The two gauged Whitespar watersheds near Prescott, Arizona, range between 1,770 and 2,135 m elevation and have a mean annual precipitation of 600 mm. The Three Bar experimental site on the Tonto National Forest includes three gauged watersheds ranging in elevation between 1,000 and 1,600 m with mean annual precipitation of 620 mm (Hibbert et al. 1982). The two sites provide 42 site-years of data and give the following rainfall–runoff relationship:

$$\begin{aligned} R &= 0.000419P^2 - 0.241P + 30.714, P \geq 385\,\text{mm} \\ r^2 &= 0.83, \text{rmse} = 14.8. \end{aligned} \quad (5)$$

To predict the baseline runoff (not accounting for the effects of restoration or fire) in a given cell of the vegetation model output, we input the precipitation for the climate scenario and year, determined as described in *Precipitation inputs*, into the equation for the forest type of the cell assigned by the vegetation model.

Equations for restoration impacts on runoff.—Forest thinning has been shown through numerous studies to increase runoff (Bosch and Hewlett 1982). To account for this, we developed forest type-specific multiple regression equations to describe the change in runoff over baseline levels due to restoration. We used data from paired watershed thinning experiments conducted at the same sites described in the previous section. Robles et al. (2014) developed the following equation for runoff increase due to restoration in ponderosa pine forest using 57 site-years of data from Beaver and Castle Creeks

$$\begin{aligned} \Delta R = & -28.464 + 0.148P - 0.015PY \\ & - 0.092P[\exp(-\mathrm{BA}_1/10.33) \\ & - \exp(-\mathrm{BA}_2/10.33)], \qquad (6) \\ & P \geq 230\,\mathrm{mm} \\ & r^2 = 0.67, \mathrm{rmse} = 25.4 \end{aligned}$$

where ΔR is the increase in annual runoff attributed to forest thinning in mm, P is total winter precipitation (October–April) in mm, Y is years since treatment, BA_1 and BA_2 are basal area before and after treatment, respectively, in m^2/ha. No increase in runoff due to thinning is predicted in years with winter precipitation below 230 mm or more than 10 yr after the thinning.

There are several assumptions inherent in this modeling approach. First, the thinning treatment conducted in the historic paired watershed studies, such as strip thinning and patch clearing, reduced basal area by a similar amount but in a different spatial pattern than modern restoration treatments. Second, it does not directly model watershed processes such as evapotranspiration and snowmelt that influence runoff. A full discussion of the model assumptions and their potential impact on results can be found in Appendix S3 of Robles et al. (2014). Process-based modeling addresses these issues, but has data input requirements and computing requirements that make it impractical for coupling with the vegetation modeling in this study. Moreno et al. (2015) used a process-based ecohydrologic model to simulate the effects of the proposed Four Forest Restoration Initiative (4FRI) on the Tonto Creek watershed in Arizona and predicted a 1–4% increase in streamflow. Robles et al. (2014) also modeled the potential effects of 4FRI using the regression approach presented here (Eq. 6) and predicted a 2% increase in streamflow. In the absence of streamflow data from restored watersheds, the agreement between these models provides converging lines of evidence that the impact of restoration on streamflow is small and positive.

Following the approach used by Robles et al. (2014), we developed an equation for change in runoff due to restoration in mixed conifer forests. We tested equations for runoff increase in mixed conifer forests with data from wet and dry mixed conifer combined and separated. The equation for combined data provided a good fit to the data, so we used the same equation for runoff increase in wet and dry mixed conifer following thinning. We fit the following equation to 22 site-years of data from Thomas and Workman Creeks:

$$\begin{aligned} \Delta R = & -16.996 + 0.0967P \\ & P[\exp(-\mathrm{BA}_1/10.33) - \exp(-\mathrm{BA}_2/10.33)], \qquad (7) \\ & r^2 = 0.86, \mathrm{rmse} = 27.9. \end{aligned}$$

We found that time since treatment was not a significant predictor of runoff increase. At the Thomas and Workman Creek sites, which were monitored for 8 and 12 yr following thinning, respectively, increased runoff was observed in thinned catchments through the duration of the study period. However, caution should be taken in applying this equation to systems more than 12 yr past thinning and as a conservative estimate we do not apply it more than 10 yr after restoration in this study.

We calculated the basal area values before and after thinning from the vegetation model as described in *Vegetation model outputs*. To predict the runoff from a ponderosa pine or mixed conifer cell in the vegetation model output that was restored within the past 10 yr, we calculated the baseline runoff with Eq. 1, 2, or 3 and added the runoff increase, calculated with Eq. 6 or 7, to the baseline.

Precipitation inputs.—We based the precipitation inputs for the equations described in the previous sections on the distribution of precipitation in the historic record to represent the high inter-annual variability that is characteristic of precipitation in the southwestern United States. We assigned precipitation inputs to vegetation model cells based on ecoregion and kept them consistent throughout model runs. For example, if a cell in the low-mid-elevation ecoregion shifted from ponderosa pine to pinyon–juniper, runoff would be calculated with the equation for pinyon–juniper (Eq. 4) and the precipitation input for the low-mid-elevation ecoregion. We used maximum likelihood estimation to fit a lognormal distribution to annual winter (October–May) precipitation data recorded at the historic paired watershed sites described in the previous sections that are representative of each ecoregion: Thomas Creek and Willow Creek for the high-elevation ecoregion, Workman Creek for the high-mid-elevation ecoregion, Beaver Creek and Castle Creek for the low-mid-elevation ecoregion, and Beaver Creek and Corduroy Creek for the low-elevation ecoregion. The two parameters of the lognormal distribution, log mean (μ) and log standard deviation (σ), for each of the ecoregions are given in Table 2. In each model run, we calculated precipitation corresponding to a given annual percentile, such as the 50th percentile to represent a median year or the 10th percentile to represent a 10-yr drought, using the cumulative distribution function of the lognormal distribution for input into the runoff equations.

We conducted runoff modeling with and without considering the effect of climate change on precipitation. This makes it possible to separate the direct effect of climate change on runoff via altered precipitation and the indirect effects of changing vegetation. The ensemble model predictions for the RCP 4.5 and 8.5 scenarios are not consistent in

Table 2. Parameters of the lognormal distribution, log mean (μ) and log standard deviation (σ), for winter (October–May) precipitation in each ecoregion and the number of site years (N) used to fit the distribution.

Ecoregion	μ	σ	N
High	6.322	0.537	52
High-mid	6.177	0.459	26
Low-mid	6.046	0.473	255
Low	5.551	0.416	69

Table 3. Change in winter precipitation (October–May) over 1990 baseline predicted by the ensemble model average under the RCP 4.5 and RCP 8.5 scenarios for the ecoregions in the study area.

	Change in winter precipitation (mm)					
	RCP 4.5			RCP 8.5		
Ecoregion	2030	2060	2090	2030	2060	2090
High	−6.7	−17.6	−16.3	0.9	−12.8	7.1
High-mid	−5.9	−15.7	−14.7	0.3	−11.5	6.4
Low-mid	−4.0	−11.7	−11.2	−0.5	−8.8	4.8
Low	−2.5	−8.0	−7.8	−0.7	−6.4	2.8

Notes: Values are an average of northeast- and southwest-facing aspects. Negative values indicate a decrease in precipitation.

their predicted trajectories for winter precipitation in the study area ecoregions (Table 3). Under the RCP 4.5 scenario, a gradual decrease in winter precipitation that stabilizes after 2060 is predicted. Very little change is predicted before 2030 for the RCP 8.5 scenario followed by a decrease up to 2060. A sharp increase between 2060 and 2090 results in 2090 values above the 1990 baseline. In cases where climate change is included in the runoff modeling, we adjusted the parameters of the lognormal distribution such that the mean of the distribution increases or decreases by the predicted change from the 1990 baseline and we do not change the standard deviation of the distribution.

Effects of fire on runoff.—High-intensity wildfire has a substantial effect on the hydrologic cycle. A number of gauged catchments in Arizona have experienced large wildfires and the records from these events suggest short-term increases in runoff (Hallema et al. 2017). Moderate to severe wildfires are also associated with substantial reductions in water quality due to increased sediment mobilization (Campbell et al. 1977, Malmon et al. 2007), so it is unlikely that runoff increases from wildfire would be beneficial to habitat or suitable for human use. Therefore, we do not model wildfire-related changes in runoff in this study. We conducted an assessment of water quality vulnerability to wildfire as described in the following section.

Sediment yield vulnerability assessment

Pelletier and Orem (2014) assessed wildfire effects on sediment yield using airborne LIDAR measurements before and one year after a major wildfire in a region of New Mexico with the same vegetation types as the Kaibab Plateau. Slope and burn severity were the main determinants of sediment yield and the following relationship was determined for sediment yield (normalized by contributing area) over contributing areas >0.1 ha:

$$Y(S,B) = 1.53S^{1.6}B^{1.7} \tag{8}$$

where Y is sediment yield (mm), S is slope (per mm), and B is equal to 1, 2, or 3 to represent the U.S. Forest Service's Burned Area Reflectance Classification (BARC) low, moderate, and high burn severities, respectively.

We applied the relationship from Pelletier and Orem (2014) to the Kaibab Plateau to identify areas that are vulnerable to water quality reductions due to wildfire. It should be noted that actual sediment yield following a wildfire depends on the frequency and intensity of rain events. Thus, the sediment yield calculations should be treated as relative values used to quantify vulnerability. We converted the burn severity estimates produced by LANDIS-II to the BARC scale as follows: (1) LANDIS-II outputs of 3 are BARC low severity, (2) LANDIS-II outputs of 4 and 5 are BARC moderate severity, and (3) LANDIS-II output 6 and 7 are BARC high severity. We calculated slope for each 1 ha vegetation model cell from the USGS National Elevation Dataset 2013 1/3 arc-second product using the ArcMap 10.3.1 Spatial Analyst Package (ESRI, Redlands, California, USA).

To quantify the impacts of stochastic fire occurrence in the LANDIS-II outputs, we calculated an expected value of annual sediment yield for each 1 ha vegetation model cell

$$\begin{aligned} E[Y_n] = {} & P_n(1)\cdot Y(S_n,1) + P_n(2)\cdot Y(S_n,2) \\ & + P_n(3)\cdot Y(S_n,3) \end{aligned} \tag{9}$$

where $E[\,\cdot\,]$ is the expected value operator; Y_n is sediment yield from the nth model cell; $P_n(1)$, $P_n(2)$, and $P_n(3)$ are the annual probability of low-, moderate-, and high-severity fire, respectively, in the nth model cell; and S_n is the slope of the nth model cell. We calculated the fire probabilities using the LANDIS-II outputs

$$P_n(B) = \frac{1}{N}\sum_{i=1}^{N}\frac{F_{B,n,i}}{L} \tag{10}$$

where N is the number of model runs, $F_{B,n,i}$ is the number of fires of severity B that occur in the nth model cell during the ith model run, and L is the length of a model run. We calculated sediment yield for the 10 model runs for the period of 1990–2060.

Results

Fire and forest modeling

Restoration treatments greatly reduced future wildfire impacts on the Kaibab Plateau under all climate scenarios. Restoration treatments decreased area burned in wildfires, with the high restoration rate nearly tripling the mean wildfire rotation (Table 4). Similarly, mean area burned in high-severity fires was greatly reduced in response to restoration treatments under all climate scenarios (Table 5). The influence of climate change on the fire regime was less pronounced, with only minor changes in fire rotation and high-severity area burned under the different climate scenarios.

Climate change resulted in marked declines in aboveground biomass (AGB). For all scenarios, mean AGB was high in 1990 due to the effects of fire exclusion during the 20th century (Fig. 1). Under the no climate change scenarios, wildfires and restoration treatments reduced biomass steadily during the 21st century to levels that approximated the historic mean exhibited during the frequent fire period. Climate change drove steeper declines in biomass beginning in the year 2030, resulting in considerable reductions in

TABLE 4. Wildfire rotation in years for Kaibab Plateau from 2010 to 2110 under potential future climate conditions and restoration rates.

Climate condition	Restoration rate: No restoration	Low restoration	High restoration
No change	45.5 (3.7)	56.4 (6.2)	123.7 (11.7)
RCP 4.5	48.1 (3.6)	63.7 (6.1)	130.8 (16.6)
RCP 8.5	41.0 (3.5)	53.3 (5.4)	127.8 (15.1)

Note: Values are means with SD in parentheses.

TABLE 5. High-severity area burned in thousands of hectares for Kaibab Plateau from 2010 to 2110 for potential future climate conditions and restoration rates.

Climate condition	Restoration rate: No restoration	Low restoration	High restoration
No change	289.0 (25.4)	207.2 (32.9)	51.6 (16.0)
RCP 4.5	229.0 (30.5)	155.2 (28.4)	45.7 (22.4)
RCP 8.5	275.1 (34.1)	187.9 (28.6)	46.8 (17.8)

Notes: Values are means with SD in parentheses. High-severity fires were fires of severity 4–5 on a scale of 1 (low-severity, surface fire) to 5 (high-severity, stand-replacing fire).

biomass by the end of the century (approximately 43–58% reduction from the historical mean). Biomass totals at the end of the climate change scenarios in 2110 were similar regardless of restoration. However, the restoration treatments did preserve biomass during the middle years of the simulation. The positive influence of restoration treatments on biomass decline was most apparent in the high climate change scenario.

The percent cover of different forests types also shifted in response to climate change (Fig. 2). Higher elevation spruce–fir, wet mixed conifer, and aspen declined under the two climate change scenarios. The high restoration scenario was most effective in retaining a higher percentage of the landscape in spruce–fir, mixed conifer, and aspen forest cover (13.5%; 13.6%) compared to low restoration (6.5%; 5.5%) and no restoration (3.8%, 3.3%), for the RCP 4.5 and RCP 8.5 climate scenarios, respectively. Non-forest area consistently increased in response to climate change. The application of restoration treatments limited this trend, with the high treatment rate most effectively reducing increases in non-forest area under both climate change scenarios.

Hydrologic modeling

In the absence of restoration, runoff in a year with median precipitation is expected to decrease by 2100 in the study area by 0.5%, 1.3%, and 10.0% for the no climate change, RCP 4.5, and RCP 8.5 scenarios, respectively, (Fig. 3) due solely to shifts in vegetation type (i.e., precipitation inputs to the hydrologic model were not adjusted to account for climate change). Restoration ameliorated the effects of runoff change due to vegetation shifts across the climate scenarios

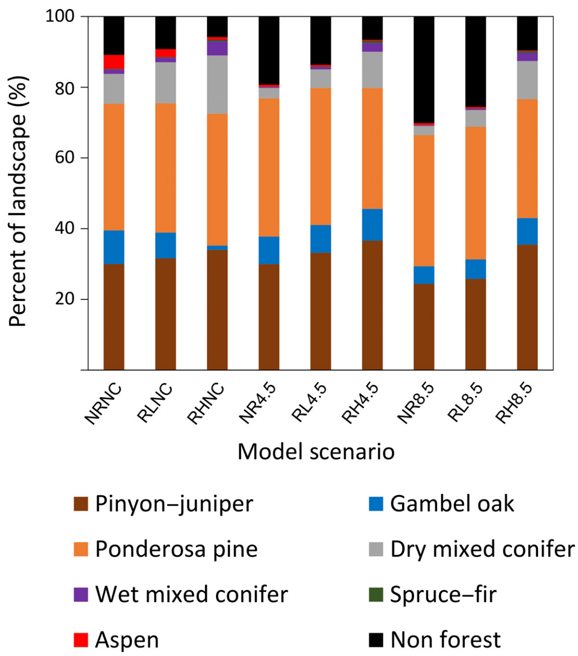

FIG. 2. Bar plot of the percentage of the study landscape in different forest types in the year 2110 under modeled climate conditions and restoration approaches (NR, no restoration; RL, low restoration; RH, high restoration; NC, no climate change; 4.5, RCP 4.5; 8.5, RCP 8.5).

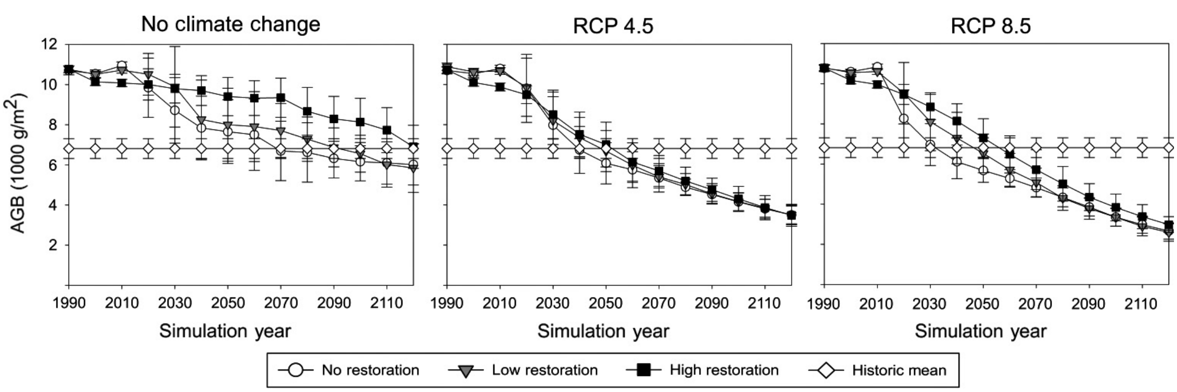

FIG. 1. Aboveground live biomass (AGB) for the Kaibab Plateau, Arizona, USA, from 1990 to 2110 under modeled future climate conditions and restoration rates. Values are mean ± SD across model runs.

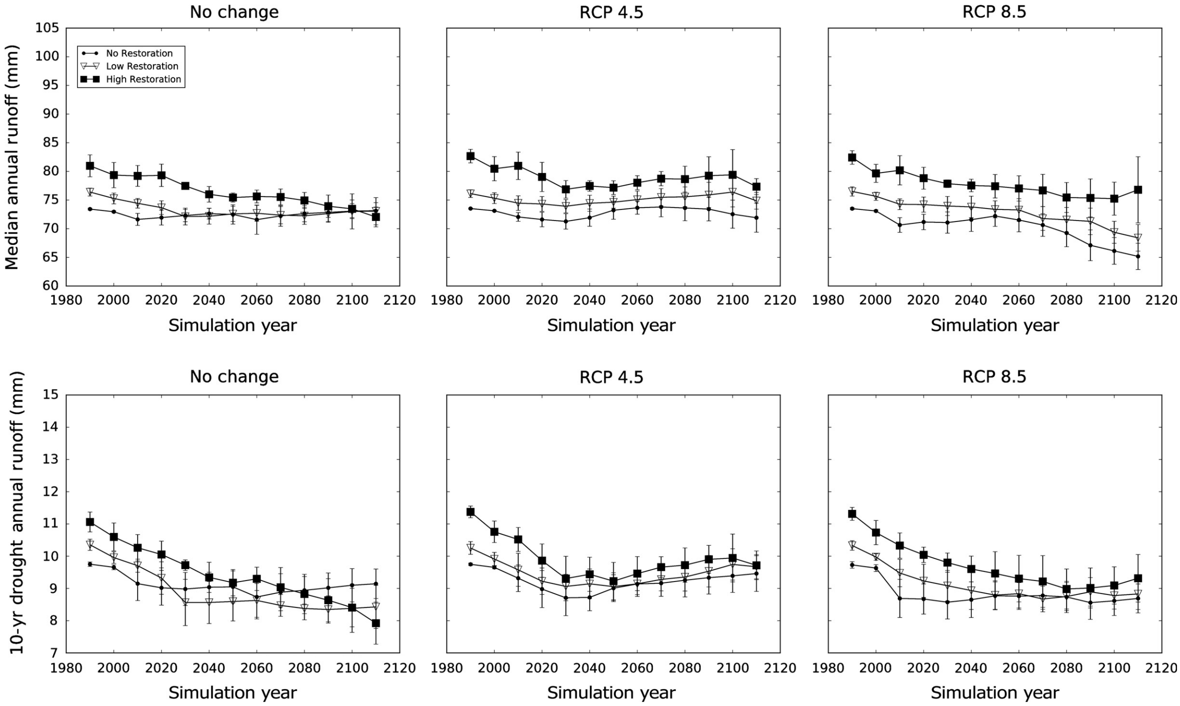

FIG. 3. Predicted total runoff from the study area, normalized by area, from 1990 to 2110 under future vegetation distributions and restoration rates. Precipitation inputs are not adjusted to account for the effects of climate change. The top row of panels shows runoff for a median (50th percentile) annual precipitation and the bottom row of panels shows runoff for a 10-yr drought (10th percentile) annual precipitation scenario. Values are means ± SD across model runs.

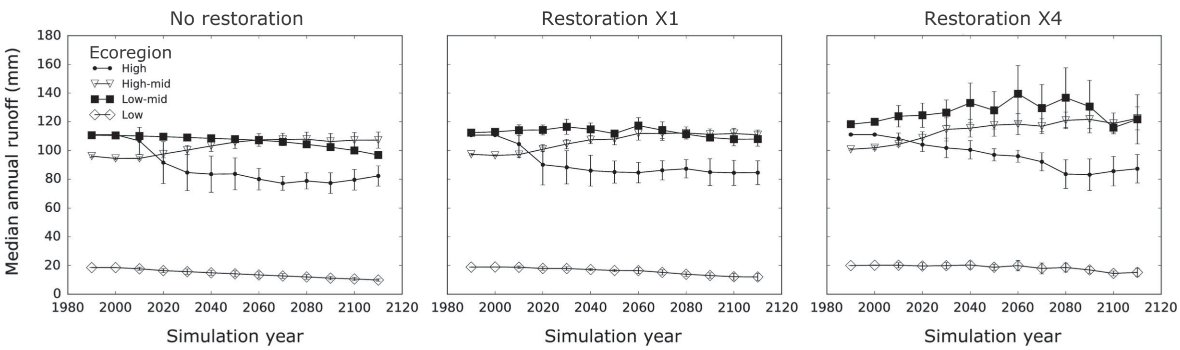

FIG. 4. Predicted runoff from each ecoregion, normalized by the area of the ecoregion, from 1990 to 2110 under the RCP 8.5 climate scenario and varying restoration rates. Precipitation inputs are not adjusted to account for the effects of climate change. Runoff is given for a median (50th percentile) annual precipitation. Values are means ± SD across model runs.

and is even expected to result in small increases (<5%) in some cases. Under drought conditions, runoff is consistently low across scenarios and is expected to decline across all climate change scenarios despite restoration treatments.

Runoff normalized by area is much higher for the forested ecoregions than for the low-elevation ecoregion that is mostly pinyon–juniper (Fig. 4). The decline in spruce–fir and wet mixed conifer forest types (Fig. 2) drives a decline in runoff in the high-elevation ecoregion by mid-century. Runoff from the high-mid-elevation ecoregion is more reliable as dry mixed conifer forests are maintained or transition to ponderosa, which has minimal consequences for runoff. Runoff from the low-elevation ecoregion declines in the RCP 4.5 and 8.5 scenarios because most low-elevation ponderosa transitions to pinyon–juniper and some pinyon–juniper transitions to non-forest. Both transitions have negative consequences for runoff.

The model estimates that under contemporary conditions, the high-mid- and low-mid-elevation ecoregions generate 81% of total runoff on the Kaibab Plateau in a median precipitation year. Though the low-elevation ecoregion is the largest by area (36% of the study area) it only contributes 9% of the total runoff from the Kaibab Plateau. The decline in runoff from high-elevation forests is driven by an increase in the frequency of years with low runoff years and a decrease in the frequency of years with moderate runoff (Fig. 5). However, years with high runoff do occur even in future scenarios under climate change.

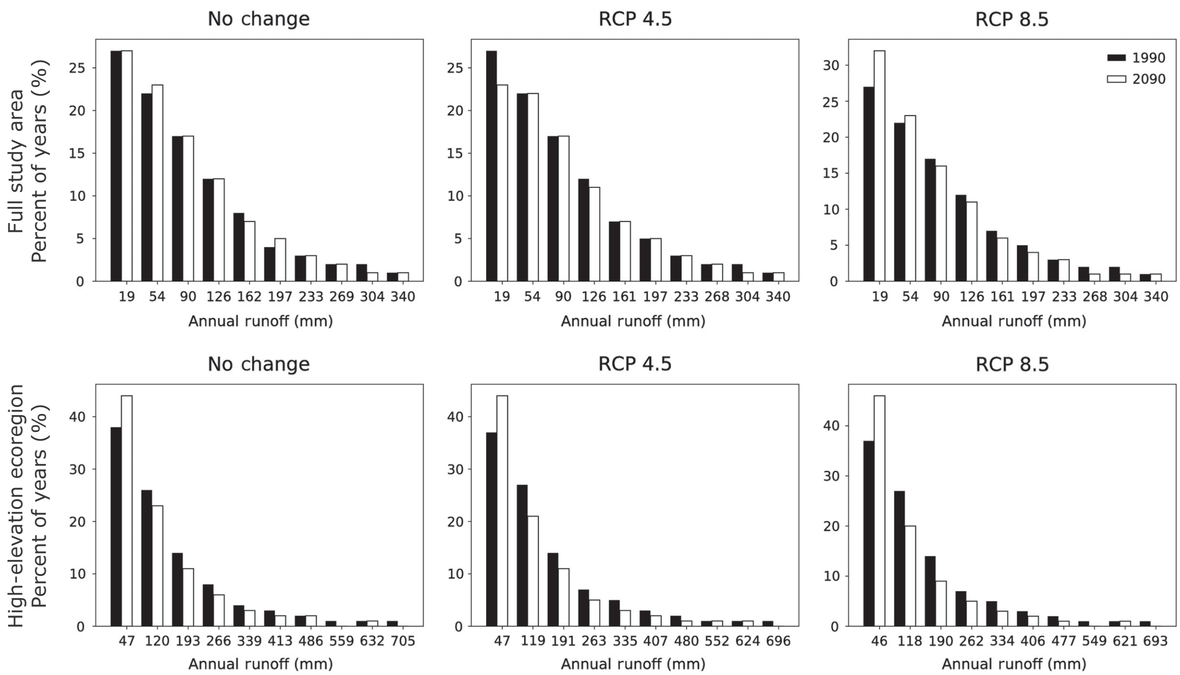

FIG. 5. Distribution of annual runoff values as the percentage of years falling in a bin centered on the given value in 1990 and 2060 under future vegetation distributions in the absence of restoration. The top panel shows averages for the entire study area and bottom panels show average values for the high-elevation ecoregion. Precipitation inputs are adjusted to account for the effects of climate change.

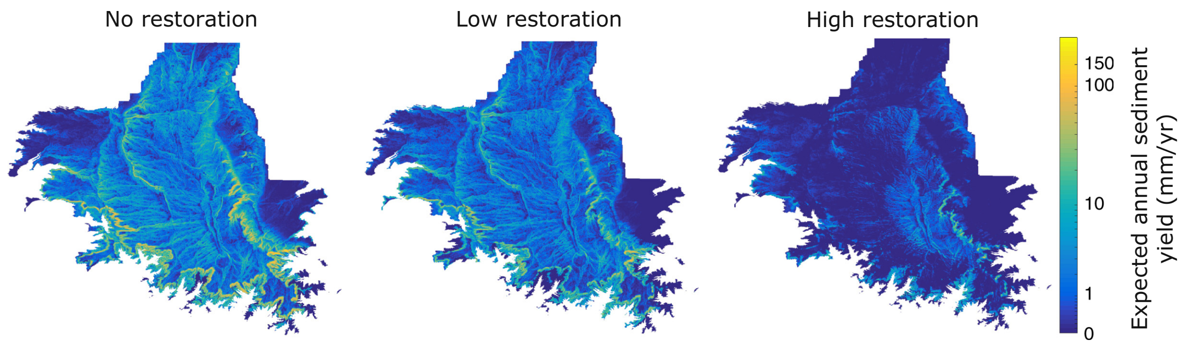

FIG. 6. Expected value of annual sediment yield between 1990 and 2060 modeled at a 1-ha scale using the annual probability of low-, moderate-, and high-severity wildfire predicted by Climate-FVS and LANDIS; slope; and the relationship between burn severity, slope, and sediment yield developed by Pelletier and Orem (2014).

Sediment yield vulnerability

Expected annual sediment yield was highest in the high-slope areas around the canyon rim and at mid elevations where fire severity was highest (Fig. 6). Sediment yield was reduced in the restoration scenarios, particularly in the mid-elevation ecoregions where most thinning activity was concentrated. Across all restoration scenarios, the low-elevation ecoregion had the highest per area sediment yield (Fig. 7). Restoration was most effective at reducing sediment yield in the low-mid- and high-mid-elevation ecoregions, where restoration treatments were applied, which had a 94% and 85% reduction, respectively, for the high restoration scenario. Even though restoration treatments were not applied in the high- and low-elevation ecoregions, there was a reduction in sediment yield of around 56% and 85%, respectively, in the high restoration scenario.

DISCUSSION

Fire regimes and forest vegetation

Climate change drove declines in AGB and shifts in forest composition; particularly the loss of higher-elevation mixed conifer, aspen, and spruce–fir forest types. In our model, forest change was primarily driven by two processes: (1) wildfire driven mortality and (2) tree regeneration failure. High-severity fire initiates change by removing AGB and necessitating forest recovery through regeneration. Under contemporary climate conditions the forest recovers relatively quickly as adjacent, unburned forests provide viable propagules that enable regeneration, biomass recovery, and compositional stability. In the case of very large patches of high-severity fire, LANDIS-II simulated regeneration delays due to the dispersal limitations of individual species propagules. However, our

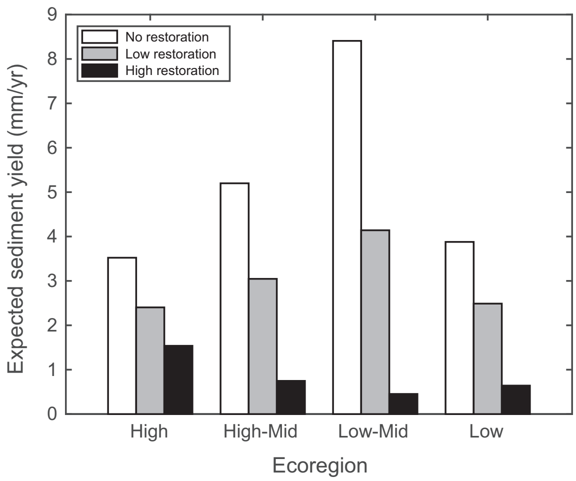

FIG. 7. Average expected annual sediment yield between 1990 and 2060 by ecoregion and restoration scenario.

implementation of LANDIS-II did not incorporate changes in soil conditions or competition with herbaceous vegetation, which can result in longer term regeneration failure following high-severity fire in southwestern forests under contemporary climate (Savage and Mast 2005, Roccaforte et al. 2012). In the climate change scenarios, the regeneration probability of adjacent species approaches zero by the middle of this century, resulting in regeneration failure and driving compositional changes. Fire disturbed sites may remain unforested for long periods until viable lower-elevation species become available for colonization through uphill migration.

Biomass declines and compositional change were greater in our study compared to recent LANDIS-II simulations of climate change in the Sierra Nevada Mountains of California (Liang et al. 2016). This may be partly due to differences in the tree species–climate relationships that drive regeneration in each study: Climate-FVS (Crookston et al. 2010) vs. Century Succession extension (Scheller et al. 2011). However, the Kaibab Plateau may be particularly vulnerable to climate induced vegetation change. The upper elevations of the plateau represent the lower end of the mesic conifer climate niche in the southwestern United States. The Kaibab Plateau does not provide cooler, higher-elevation habitat where these species might be less vulnerable to climate change. Our results are similar to other bioclimatic models that project the decline of *P. engelmannii* and *P. menziesii* on the Kaibab Plateau (Notaro et al. 2012, Truettner 2013, Rehfeldt et al. 2014). The Sierra Nevada Mountains or the more southerly Pinaleño Mountains in Arizona and Sangre de Cristo Mountains in New Mexico may provide higher-elevation habitat that supports greater retention or uphill migration of spruce–fir, mixed conifer, and aspen.

Restoration treatments, through their effects on the fire regime, mediated climate-driven changes in vegetation. Previous empirical and modeling studies have shown that landscape scale restoration can have a significant impact on area burned and fire severity in southwestern forests (Finney et al. 2005, Fulé et al. 2012, Hurteau 2017). In our simulations, restoration treatments effectively reduced area burned regardless of climate scenario. Indeed the climate condition had limited influence on the fire regime, suggesting that in our model fire was driven more by fuel condition, rather than fire weather. Reductions in high-severity area burned due to the restoration treatments reduced turnover of high-elevation forest types and reduced non-forest area. While the loss of climate conditions conducive to the regeneration of mesic conifers and aspen indicates that they will eventually be lost from the plateau (Flatley and Fulé 2016), in the absence of stand replacing disturbances, tree longevity enables overstory forest vegetation change to lag behind climate change (Svenning and Sandel 2013). Therefore wildfire, in addition to insect, disease, and drought mortality, will modify the timing of forest turnover and consequent climate-induced vegetation change. Our models suggest that forest restoration can delay vegetation change, reducing the steepness of biomass declines and providing opportunities for uphill movement of lower-elevation species.

The hydrologic modeling suggests that a decrease in total runoff from the Kaibab Plateau of up to 10% could be possible without restoration. Even though conservative assumptions were used with regards to runoff increases, restoration resulted in small increases in runoff in most cases. The increases were not large enough to plan for increased runoff following restoration. This is consistent with results from other landscape-scale modeling studies of restoration impacts on hydrology (Robles et al. 2014, Moreno et al. 2015). However, larger decreases in runoff are expected for areas in the high- and low-elevation ecoregions under all scenarios, though the declines are greatest without restoration. This poses a particular concern for a karst system such as the Kaibab Plateau, because the source area of a spring may be localized within one ecoregion. Flow reductions at high elevation are of greater concern for springs, because sinkhole density is positively correlated with elevation and with geologic structure (Jones et al. 2017). Flow in Roaring Spring, the water supply for GCNP, is a combination of rapid flow through conduits in the Karst geology and slow flow through a low-permeability matrix. Rapid flow travels 2,000 m vertically and over 40 km horizontally in less than six weeks (Jones et al. 2017). Because the water from rapid flow is so young, increases in sediment yield on the Kaibab Plateau are likely to increase turbidity in Roaring Spring.

The model results for the high-elevation ecoregion should be interpreted cautiously. Data on rainfall–runoff relationships for non-forested areas, which account for a significant portion of the ecoregion by the end of the simulation, are limited in high-elevation regions, so we applied a relationship for non-forested areas at lower elevations. Historical studies showing runoff increases following clearcutting (Baker 1986) suggest that runoff may increase following forest canopy loss due to successional changes, which is opposite of what is predicted by our modeling framework. Data from high-elevation forests in Wyoming affected by Mountain Pine Beetle found that runoff decreased substantially relative to a control site when forest canopy was lost (Biederman et al. 2014), and a broader analysis of sites affected by tree die-off found no change or a decrease in runoff (Biederman et al. 2015). This suggests that forest loss due to die-off and successional change, which is what we predict will happen on the Kaibab Plateau, has a fundamentally different impact on the hydrologic cycle than logging.

Restoration was highly effective in reducing the vulnerability of the entire study area to sediment yield following wildfire. Restoration treatments impacted sediment yield most clearly in the mid-elevation zones where treatments were carried out. However, it also reduced sediment yield in the more vulnerable low- and high-elevation ecoregions, presumably by reducing the likelihood of high-severity fire spreading into these untreated forest types. The impact of restoration on sediment yield was much greater than the impact on runoff, suggesting that the primary hydrologic benefit of restoration projects is to reduce the vulnerability of the water supply to increased turbidity following wildfire.

Conclusions

Our results indicated that a high restoration rate (20-yr prescribed burning rotation) was the most beneficial in terms of reducing high-severity fire, slowing forest composition change, maintaining runoff, and reducing sediment yield. The lower restoration rate (80-yr prescribed burning rotation) provided some positive benefits, which supports the implementation of more limited restoration projects, when funding for more extensive or frequent treatments is not feasible. Prescribed burning rotations shorter than 20 yr may be inadvisable, driving more rapid declines of contemporary forests and preventing uphill migration of species adapted to the new climate regime (Diggins et al. 2010, Flatley and Fulé 2016). High-elevation forests were most vulnerable to reductions in water yield due to climate change. Consistent with other landscape-scale studies, restoration resulted in only small increases in runoff but was effective in minimizing reductions in runoff due to climate change. Our simulations indicate that restoration is an effective tool for preventing erosion and water quality issues associated with high-severity wildfire.

Acknowledgments

This research was funded by the Bureau of Reclamation WaterSMART: Applied Science Grants for the Southern Rockies Landscape Conservation Cooperative agreement R14AC00082. Additional funding was provided by the Northern Arizona University Technology and Research Initiative Fund and the Nature Conservancy in New Mexico.

Literature Cited

Allen, C. D., and D. D. Breshears. 1998. Drought-induced shift of a forest-woodland ecotone: rapid landscape response to climate variation. Proceedings of the National Academy of Sciences USA 95:14839–14842.

Baker, M. B. 1986. Effects of ponderosa pine treatments on water yield in Arizona. Water Resources Research 22:67–73.

Baker, M. B. 1999. History of watershed research in the Central Arizona Highlands. U.S. Department of Agriculture, Forest Service, Rocky Mountain Research Station, Flagstaff, Arizona, USA.

Barr, G. W. 1956. Recovering rainfall. Department of Agricultural Economics, University of Arizona, Tucson, Arizona, USA.

Biederman, J. A., A. A. Harpold, D. J. Gochis, B. E. Ewers, D. E. Reed, S. A. Papuga, and P. D. Brooks. 2014. Increased evaporation following widespread tree mortality limits streamflow response. Water Resources Research 50:5395–5409.

Biederman, J. A., A. J. Somor, A. A. Harpold, E. D. Gutmann, D. D. Breshears, P. A. Troch, D. J. Gochis, R. L. Scott, A. J. H. Meddens, and P. D. Brooks. 2015. Recent tree die-off has little effect on streamflow in contrast to expected increases from historical studies. Water Resources Research 51:9775–9789.

Bosch, J., and J. Hewlett. 1982. A review of catchment experiments to determine the effect of vegetation changes on water yield and evapotranspiration. Journal of Hydrology 55:3–23.

Brown, C. 2011. Physical, geochemical, and isotopic analyses of R-aquifer springs, North Rim, Grand Canyon. Thesis. Northern Arizona University, Flagstaff, Arizona, USA.

Campbell, R. E., M. B. Baker, P. F. Ffolliott, F. R. Larson, and C. Avery. 1977. Wildfire effects on a ponderosa pine ecosystem: an Arizona case study. Research Paper RM-191, USDA Forest Service, Fort Collins, Colorado, USA.

Chojnacky, D. C., L. S. Heath, and J. C. Jenkins. 2014. Updated generalized biomass equations for North American tree species. Forestry 87:129–151.

Clary, W. P., M. B. Baker Jr., P. F. O'Connell, T. N.Johnson Jr., and R. E. Campbell. 1974. Effects of pinyon–juniper removal on natural resource products and uses in Arizona. Research Paper RM-128, USDA Forest Service, Fort Collins, Colorado, USA.

Collings, M., and R. Myrick. 1966. Effects of juniper and pinyon eradication on streamflow from Corduroy Creek basin, Arizona. USGS Numbered Series 491-B. U.S. Government Printing Office, Washington, District of Columbia, USA.

Crookston, N. L., and G. E. Rehfeldt. 2008. Climate estimates and plant–climate relationships. USDA Forest Service, Rocky Mountain Research Station, Moscow, Idaho, USA.

Crookston, N. L., G. E. Rehfeldt, G. E. Dixon, and A. R. Weiskittel. 2010. Addressing climate change in the forest vegetation simulator to assess impacts on landscape forest dynamics. Forest Ecology and Management 260:1198–1211.

Diggins, C., P. Z. Fulé, J. P. Kaye, and W. W. Covington. 2010. Future climate affects management strategies for maintaining forest restoration treatments. International Journal of Wildland Fire 19:903–913.

Duveneck, M. J., and R. M. Scheller. 2015. Climate-suitable planting as a strategy for maintaining forest productivity and functional diversity. Ecological Applications 25:1653–1668.

Earl, S. R., and D. W. Blinn. 2003. Effects of wildfire ash on water chemistry and biota in South-Western U.S.A. streams. Freshwater Biology 48:1015–1030.

Finney, M. A., C. W. McHugh, and I. C. Grenfell. 2005. Stand- and landscape-level effects of prescribed burning on two Arizona wildfires. Canadian Journal of Forest Research 35:1714–1722.

Flatley, W. T., and P. Z. Fulé. 2016. Are historical fire regimes compatible with future climate? Implications for forest restoration. Ecosphere 7:e01471.

Fulé, P. Z., W. W. Covington, M. M. Moore, T. A. Heinlein, and A. E. Waltz. 2002. Natural variability in forests of the Grand Canyon, USA. Journal of Biogeography 29:31–47.

Fulé, P. Z., J. E. Crouse, T. A. Heinlein, M. M. Moore, W. W. Covington, and G. Verkamp. 2003*a*. Mixed-severity fire regime in a high-elevation forest of Grand Canyon, Arizona, USA. Landscape Ecology 18:465–486.

Fulé, P. Z., T. A. Heinlein, W. W. Covington, M. M. Moore, P. Z. Fulé, T. A. Heinlein, W. W. Covington, and M. M. Moore. 2003*b*. Assessing fire regimes on Grand Canyon landscapes with fire-scar and fire-record data. International Journal of Wildland Fire 12:129–145.

Fulé, P. Z., J. E. Crouse, J. P. Roccaforte, and E. L. Kalies. 2012. Do thinning and/or burning treatments in western USA ponderosa or Jeffrey pine-dominated forests help restore natural fire behavior? Forest Ecology and Management 269:68–81.

Golladay, S. W., K. L. Martin, J. M. Vose, D. N. Wear, A. P. Covich, R. J. Hobbs, K. D. Klepzig, G. E. Likens, R. J. Naiman, and A. W. Shearer. 2016. Achievable future conditions as a framework for guiding forest conservation and management. Forest Ecology and Management 360:80–96.

Gottfried, G. J. 1983. Stand changes on a southwestern mixed conifer watershed after timber harvesting. Journal of Forestry 81:311–316.

Gottfried, G. J. 1991. Moderate timber harvesting increases water yields from an Arizona mixed conifer watershed. JAWRA Journal of the American Water Resources Association 27:537–546.

Gustafson, E. J., S. R. Shifley, D. J. Mladenoff, K. K. Nimerfro, and H. S. He. 2000. Spatial simulation of forest succession and timber harvesting using LANDIS. Canadian Journal of Forest Research 30:32–43.

Gustafson, E. J., A. Z. Shvidenko, B. R. Sturtevant, and R. M. Scheller. 2010. Predicting global change effects on forest biomass and composition in south-central Siberia. Ecological Applications 20:700–715.

Hallema, D. W., G. Sun, K. D. Bladon, S. P. Norman, P. V. Caldwell, Y. Liu, and S. G. McNulty. 2017. Regional patterns of postwildfire streamflow response in the Western United States: the importance of scale-specific connectivity. Hydrological Processes 31:2582–2598.

Hibbert, A. R., E. A. Davis, and O. D. Knipe. 1982. Water yield changes resulting from treatment of Arizona chaparral. General Technical Report PSW-58. Pages 382–389 U.S. Department of Agriculture, Forest Service, Berkeley, California, USA.

Huffman, D. W., P. Z. Fule, J. E. Crouse, and K. M. Pearson. 2009. A comparison of fire hazard mitigation alternatives in pinyon–juniper woodlands of Arizona. Forest Ecology and Management 257:628–635.

Huffman, D. W., P. Z. Fulé, K. M. Pearson, and J. E. Crouse. 2008. Fire history of pinyon–juniper woodlands at upper ecotones with ponderosa pine forests in Arizona and New Mexico. Canadian Journal of Forest Research 38:2097–2108.

Hurteau, M. D. 2017. Quantifying the carbon balance of forest restoration and wildfire under projected climate in the fire-prone southwestern US. PLoS ONE 12:e0169275.

Hurteau, M. D., S. Liang, K. L. Martin, M. P. North, G. W. Koch, and B. A. Hungate. 2016. Restoring forest structure and process stabilizes forest carbon in wildfire-prone southwestern ponderosa pine forests. Ecological Applications 26:382–391.

Huxman, T. E., B. P. Wilcox, D. D. Breshears, R. L. Scott, K. A. Snyder, E. E. Small, K. Hultine, W. T. Pockman, and R. B. Jackson. 2005. Ecohydrological implications of woody plant encroachment. Ecology 86:308–319.

Jones, C. J. R., A. E. Springer, B. W. Tobin, S. J. Zappitello, and N. A. Jones. 2017. Hydraulic response of the shallow and deep Karst Systems of the Kaibab Plateau and Grand Canyon National Park as revealed by dye tracing and recession analysis. Advances in karst research: theory, fieldworrk and application. Geological Society, London, Special Publications 466:237–260.

Lauber, U., and N. Goldscheider. 2014. Use of artificial and natural tracers to assess groundwater transit-time distribution and flow systems in a high-alpine karst system (Wetterstein Mountains, Germany). Hydrogeology Journal 22:1807–1824.

Liang, S., M. D. Hurteau, and A. L. Westerling. 2016. Response of Sierra Nevada forests to projected climate–wildfire interactions. Global Change Biology 23:2016–2030.

Mahler, B. J., J.-C. Personné, F. L. Lynch, and P. C. V. Metre. 2004. Sediment and sediment-associated contaminant transport through Karst. Pages 23–46 *in* I. D. Sadowsky and J. Mylroie, editors. Studies of cave sediments. Springer, New York, New York, USA.

Malmon, D. V., S. L. Reneau, D. Katzman, A. Lavine, and J. Lyman. 2007. Suspended sediment transport in an ephemeral stream following wildfire. Journal of Geophysical Research: Earth Surface 112:F02006.

Meinshausen, M., et al. 2011. The RCP greenhouse gas concentrations and their extensions from 1765 to 2300. Climatic Change 109:213–241.

Monroe, S. A., R. C. Antweiler, R. J. Hart, H. E. Taylor, M. Truini, J. R. Rihs, and T. J. Felger. 2004. Chemical characteristics of ground-water discharge along the south rim of Grand Canyon in Grand Canyon National Park, Arizona, 2000–2001. USGS Scientific Investigations 5146. U.S. Geological Survey, Reston, Virginia, USA.

Moreno, H. A., H. V. Gupta, D. D. White, and D. A. Sampson. 2015. Modeling the distributed effects of forest thinning on the long-term water balance and stream flow extremes for a semi-arid basin in the southwestern US. Hydrology and Earth System Sciences Discussions 12:10827–10891.

Neary, D. G., G. G. Ice, and C. R. Jackson. 2009. Linkages between forest soils and water quality and quantity. Forest Ecology and Management 258:2269–2281.

Neary, D. G., K. A. Koestner, A. Youberg, and P. E. Koestner. 2012. Post-fire rill and gully formation, Schultz Fire 2010, Arizona, USA. Geoderma 191:97–104.

NOAA NCEI. 2011. 1981–2010 U.S. climate normals. National Oceanic and Atmospheric Administration, National Centers for Environmental Information, Asheville, North Carolina, USA.

Notaro, M., A. Mauss, and J. W. Williams. 2012. Projected vegetation changes for the American Southwest: combined dynamic modeling and bioclimatic-envelope approach. Ecological Applications 22:1365–1388.

Pelletier, J. D., and C. A. Orem. 2014. How do sediment yields from post-wildfire debris-laden flows depend on terrain slope, soil burn severity class, and drainage basin area? Insights from airborne-LiDAR change detection. Earth Surface Processes and Landforms 39:1822–1832.

PRISM Climate Group. 2004. Oregon State University. http://prism.oregonstate.edu

Rehfeldt, G. E., B. C. Jaquish, J. López-Upton, C. Sáenz-Romero, J. B. St Clair, L. P. Leites, and D. G. Joyce. 2014. Comparative genetic responses to climate for the varieties of *Pinus ponderosa* and *Pseudotsuga menziesii*: realized climate niches. Forest Ecology and Management 324:126–137.

Reynolds, R. T., A. J. S. Meador, J. A. Youtz, T. Nicolet, M. S. Matonis, P. L. Jackson, D. G. DeLorenzo, and A. D. Graves. 2013. Restoring composition and structure in Southwestern frequent-fire forests: a science-based framework for improving ecosystem resiliency. General Technical Report RMRS-GTR-310. USDA Forest Service, Fort Collins, Colorado, USA.

Rich, L. R. 1972. Managing a Ponderosa pine forest to increase water yield. Water Resources Research 8:422–428.

Rich, L. R., and G. J. Gottfried. 1976. Water yields resulting from treatments on the Workman Creek Experimental Watersheds in central Arizona. Water Resources Research 12:1053–1060.

Robles, M. D., R. M. Marshall, F. O'Donnell, E. B. Smith, J. A. Haney, and D. F. Gori. 2014. Effects of climate variability and accelerated forest thinning on watershed-scale runoff in southwestern USA ponderosa pine forests. PLoS ONE 9:e111092.

Robles, M. D., D. S. Turner, and J. A. Haney. 2017. A century of changing flows: forest management changed flow magnitudes and warming advanced the timing of flow in a southwestern US river. PLoS ONE 12:e0187875.

Roccaforte, J. P., P. Z. Fulé, W. W. Chancellor, and D. C. Laughlin. 2012. Woody debris and tree regeneration dynamics following severe wildfires in Arizona ponderosa pine forests. Canadian Journal of Forest Research 42:593–604.

Ross, L. E. 2005. Interpretive three-dimensional numerical groundwater flow modeling, Roaring Springs, Grand Canyon, Arizona. Dissertation. Northern Arizona University, Flagstaff, Arizona, USA.

Savage, M., and J. N. Mast. 2005. How resilient are southwestern ponderosa pine forests after crown fires? Canadian Journal of Forest Research 35:967–977.

Scanlon, B. R., R. C. Reedy, D. A. Stonestrom, D. E. Prudic, and K. F. Dennehy. 2005. Impact of land use and land cover change on groundwater recharge and quality in the southwestern US. Global Change Biology 11:1577–1593.

Scheller, R. M., J. B. Domingo, B. R. Sturtevant, J. S. Williams, A. Rudy, E. J. Gustafson, and D. J. Mladenoff. 2007. Design, development, and application of LANDIS-II, a spatial landscape simulation model with flexible temporal and spatial resolution. Ecological Modelling 201:409–419.

Scheller, R. M., D. Hua, P. V. Bolstad, R. A. Birdsey, and D. J. Mladenoff. 2011. The effects of forest harvest intensity in combination with wind disturbance on carbon dynamics in Lake States Mesic Forests. Ecological Modelling 222:144–153.

Scheller, R. M., and D. J. Mladenoff. 2004. A forest growth and biomass module for a landscape simulation model, LANDIS: design, validation, and application. Ecological Modelling 180:211–229.

Schindel, G. M. 2015. Determining groundwater residence times of the Kaibab Plateau, R-Aquifer using temperature, Grand Canyon National Park, Arizona. Dissertation. Northern Arizona University, Flagstaff, Arizona, USA.

Sesnie, S., and J. Bailey. 2003. Using history to plan the future of old-growth Ponderosa Pine. Journal of Forestry 101:40–47.

Smith, H. G., G. J. Sheridan, P. N. J. Lane, P. Nyman, and S. Haydon. 2011. Wildfire effects on water quality in forest catchments: a review with implications for water supply. Journal of Hydrology 396:170–192.

Stephenson, N. L. 2014. Making the transition to the third era of natural resources management. George Wright Forum 31:227.

Strom, B. A., and P. Z. Fulé. 2007. Pre-wildfire fuel treatments affect long-term ponderosa pine forest dynamics. International Journal of Wildland Fire 16:128–138.

Sturtevant, B. R., R. M. Scheller, B. R. Miranda, D. Shinneman, and A. Syphard. 2009. Simulating dynamic and mixed-severity fire regimes: a process-based fire extension for LANDIS-II. Ecological Modelling 220:3380–3393.

Svenning, J.-C., and B. Sandel. 2013. Disequilibrium vegetation dynamics under future climate change. American Journal of Botany 100:1266–1286.

Tarancón, A. A., P. Z. Fulé, K. L. Shive, C. H. Sieg, A. S. Meador, and B. Strom. 2014. Simulating post-wildfire forest trajectories under alternative climate and management scenarios. Ecological Applications 24:1626–1637.

Tobin, B. W., A. E. Springer, D. K. Kreamer, and E. Schenk. 2017. The distribution, flow, and quality of Grand Canyon Springs, Arizona (USA). Hydrogeology 26:1–12.

Truettner, C. M. 2013. Spruce–fir forest decline in the southwestern USA: species distribution modeling meets ecological realism. Dissertation. Northern Arizona University, Flagstaff, Arizona, USA.

USDA NRCS. 2013. Soil survey geographic (SSURGO) database for Coconino County Area, Arizona, North Kaibab part. U.S. Department of Agriculture, Natural Resources Conservation Service, Fort Worth, Texas, USA.

Vankat, J. L. 2011*a*. Post-1935 changes in forest vegetation of Grand Canyon National Park, Arizona, USA: part 1-ponderosa pine forest. Forest Ecology and Management 261:309–325.

Vankat, J. L. 2011*b*. Post-1935 changes in forest vegetation of Grand Canyon National Park, Arizona, USA: part 2-Mixed conifer, spruce–fir, and quaking aspen forests. Forest Ecology and Management 261:326–341.

Vesper, D. J., C. M. Loop, and W. B. White. 2001. Contaminant transport in karst aquifers. Theoretical and Applied Karstology 13:101–111.

Westerling, A. L., M. G. Turner, E. A. H. Smithwick, W. H. Romme, and M. G. Ryan. 2011. Continued warming could transform Greater Yellowstone fire regimes by mid-21st century. Proceedings of the National Academy of Sciences USA 108: 13165–13170.

Woodhouse, C. A., D. M. Meko, G. M. MacDonald, D. W. Stahle, and E. R. Cook. 2010. A 1,200-year perspective of 21st century drought in southwestern North America. Proceedings of the National Academy of Sciences USA 107:21283–21288.

Wyatt, C. J. 2013. Estimating aquifer response following forest restoration and climate change along the Mogollon Rim, northern Arizona. Dissertation. Northern Arizona University, Flagstaff, Arizona, USA.

Wyatt, C. J., F. C. O'Donnell, and A. E. Springer. 2015. Semi-arid aquifer responses to forest restoration treatments and climate change. Groundwater 53:207–216.

Yocom, L. L. 2013. Fuel treatment longevity: a summary of the science. Working Papers in Southwestern Ponderosa Pine Forest Restoration 27. Published by Southwest Fire Science Consortium and Ecological Restoration Institute, Flagstaff, Arizona, USA.

Supporting Information

Additional supporting information may be found online at: http://onlinelibrary.wiley.com/doi/10.1002/eap.1746/full